JOURNAL OF CATALYSIS **142**, 572–584 (1993)

Kinetic and Infrared Spectroscopic Studies of Fe–Y Zeolites for the Selective Catalytic Reduction of Nitric Oxide by Ammonia

M. D. AMIRIDIS,* F. PUGLISI, J. A. DUMESIC,*[1] W. S. MILLMAN,†
AND NAN-YU TOPSØE‡

**Chemical Engineering Department, University of Wisconsin, Madison, Wisconsin 53706; †Department of Chemistry, University of Wisconsin, P.O. Box 413, Milwaukee, WI 53201; and ‡Haldor Topsoe Research Laboratories, DK-2000, Lyngby, Denmark*

Received February 16, 1993; revised March 25, 1993

Reaction kinetics and infrared spectroscopic studies of the selective catalytic reduction of nitric oxide by ammonia were conducted at reactant concentrations near 500 ppm and temperatures from 473 to 623 K, over Fe–Y zeolites having Si/Al ratios of 2.4, 3.2, and 4.4. The presence of iron cations within the zeolite was necessary to sustain steady-state catalytic activity, which was enhanced by about two orders of magnitude in the presence of oxygen. The reaction was near first order in NO and near zero order in ammonia. Ammonia oxidation was found to become a significant competing reaction between 493 and 543 K over zeolites with Si/Al ratios equal to 2.4 and 3.2. Ammonia oxidation did not occur over the sample with a Si/Al ratio of 4.4. The primary surface species observed under reaction conditions by *in situ* IR spectroscopy were NH_3 and NH_4^+. In the absence of oxygen, the rate-limiting step appears to be the reoxidation of iron. © 1993 Academic Press, Inc.

INTRODUCTION

The catalytic reduction of NO is of importance for the control of emissions from stationary sources, such as flue gases from combustion units. Ammonia is a useful reducing agent for this reaction, due to its high selectivity for the reduction of NO in the presence of O_2. Different metals, metal oxides, and zeolites have been used in kinetic studies of the selective catalytic reduction (SCR) of nitric oxide by ammonia. Of these catalysts, vanadia/titania is one of the best because of its high activity and its resistance to poisoning by SO_x (e.g., (*1–8*)). Although not as selective as vanadium oxide, iron oxide also exhibits significant activity for NO reduction by ammonia. Furthermore, the kinetic parameters reported for iron oxide are not significantly different from those reported for vanadia (*5–9*). In addition, Co- and Cu-exchanged Y zeolites have been studied for the SCR reaction (*10–15*). The kinetic parameters observed over these catalysts at temperatures near 400 K have been reported to be different from those measured over corresponding metal oxide catalysts.

In this paper we report the results of kinetic and infrared spectroscopic studies of the selective catalytic reduction of NO by NH_3 over Fe–Y zeolites. In particular, we have studied Fe–Y zeolites with differing Si/Al ratios, because these materials combine the high activity of iron oxide for the SCR reaction and the unique structural properties of the zeolite framework. The isolation of exchange cations in the zeolite framework provides an opportunity to study the catalytic properties of these cations in a well-defined environment. Infrared spectroscopy was used to monitor the chemical species adsorbed on the catalyst surface under SCR reaction conditions and after different catalyst pretreatments. Similar *in situ* IR studies of nitric oxide reduction over titania (*16*), vanadia/titania (*17*) and Co–Y zeolites

---

[1] To whom correspondence should be addressed.

0021-9517/93 $5.00

TABLE 1

Chemical Analysis Results for Fe–Y Zeolites (Dry Basis)

Si/Al ratio	Fe content (Fe cations/g)
2.4	7.3×10^{20}
3.2	5.6×10^{20}
4.4	4.6×10^{20}

(*15–18*) have been reported. We have also utilized *in situ* Mössbauer spectroscopy to monitor the changes in iron oxidation states during the SCR reaction. Results from those studies were reported earlier (*19*). These spectroscopic studies enhance our understanding by providing information concerning the state of the active metal cations and the adsorbed species present on the surface under the conditions at which kinetic measurements are obtained.

EXPERIMENTAL

The starting material for the varying Si/Al ratio Y-zeolites used here was Linde SK-40 (lot no. 1280-133) with a Si/Al ratio of 2.4. The 3.2 and 4.4 Si/Al ratio samples were prepared by reacting $(NH_4)_2SiF_6$ with an aqueous suspension of Na–Y. Ferrous cations were exchanged into the zeolites using $FeSO_4$ in aqueous solution under a nitrogen atmosphere (*20*). During the exchange process the solution pH was maintained between 3.8 and 4.0 to prevent hydrolysis of the zeolite at lower pH and the formation of iron hydroxide at higher pH. The Si/Al ratios and iron contents were determined by chemical analysis (Galbraith Laboratories), the results of which are shown in Table 1.

Steady-state kinetic studies were conducted using a glass flow reactor. Helium (Liquid Carbonics) was purified by passing through copper turnings at 473 K and a molecular sieve trap at 77 K. Oxygen (Liquid Carbonic) was purified by passage through a molecular sieve trap at 195 K. Gases used for SCR kinetic studies were mixed from three certified analyzed mixtures of 1000–1100 ppm NO in He, 1000–1100 ppm NH_3 in He (Matheson or AGA), and 5% O_2 in He (AGA). Helium was added when necessary to dilute further the reacting gas mixture. The NH_3 in He was used without further purification. The NO in He was passed through a glass bead trap at 195 K. The O_2 in He was purified in the same manner as the O_2 mentioned above.

The reacting gases were mixed prior to the reactor entrance and preheated to the reaction temperature by passage through a glass coil. A thermocouple well in the center of the catalyst bed was used to measure the catalyst temperature. The inlet and reactor effluent gases were analyzed by chemiluminescence for NO (Model 10A Thermo Electron Analyzer) and acidic titration for NH_3. The reactor effluent gas was periodically trapped and analyzed by infrared spectroscopy to estimate the concentration of N_2O produced. Prior to the introduction on the reacting gas mixture, the samples were heated in He to 673 K and then treated at this temperature for 4 h in flowing O_2 (200 cm^3/min).

Infrared spectra were collected using a Nicolet model 170SX Fourier transform spectrometer equipped with a narrow-band MCT detector. Transmission spectra were collected in the single beam mode. Reference spectra of the clean surfaces were collected separately and the data shown herein are the difference between the sample and the reference. A stainless steel IR cell with a 15-cm path length having KBr windows was used. A heating element wrapped around the cell allowed collection of *in situ* spectra at temperatures up to 623 K. For experiments at elevated temperatures, the windows were cooled by flowing water through copper tubing curved around the windows. Samples were self-supporting wafers that had a diameter of 2.5 cm and a thickness of about 5 mg/cm^2. The infrared studies were conducted with the same gases used for the kinetic studies.

TABLE 2

Catalytic Activities for Fe–Y Zeolites in the Absence of O_2

Si/Al ratio	Rate[a]	TOF[b]	E_{ACT}[c]
2.4	2.1×10^{15}	2.9×10^{-6}	31.0[d]
3.2	1.6×10^{15}	2.9×10^{-6}	68.5[e]
4.4	6.6×10^{14}	1.5×10^{-6}	44.0[f]

[a] Estimated at 523 K, 600 ppm NO, 400 ppm NH_3. Units of molecules of NO/g of catalyst/s.

[b] Estimated at 523 K, 600 ppm NO, 400 ppm NH_3. Units of molecules of NO/Fe cation/s.

[c] Activation Energy (kJ/mol).

[d] Temperature range of 545–655 K.

[e] Temperature range of 540–630 K.

[f] Temperature range of 580–675 K.

RESULTS

Two NaH–Y zeolites having Na contents corresponding to 17 and 34% of the ion-exchange capacity and with a Si/Al ratio of 2.4 were examined for their activity towards SCR at 523 K in the presence of oxygen. No measurable NO consumption was found for these samples, which contained 400 ppm of iron as an impurity.

Catalytic Behavior in the Absence of Oxygen

Catalytic activities were obtained in the absence of O_2 over a temperature range from 545 to 675 K. All initially oxidized Fe–Y catalysts exhibited deactivation extending over a period of 20 to 30 h. During this period, the activity decreased by nearly two orders of magnitude. Mössbauer spectroscopy (*19*) has shown this loss in activity to be related to the reduction of ferric to ferrous iron. Rate measurements of the apparent steady state reached following the deactivation period were carried out at various temperatures with 600 ppm of NO and 400 ppm of NH_3. These data are summarized in Table 2, which lists the rate of NO reduction, the turnover frequency (TOF), and the activation energy for each Fe–Y zeolite. Comparison of the TOF values of these zeolites with typical values reported for vanadium oxide catalysts (*1, 2, 21, 22*) shows the iron zeolites to be between two and eight times less active. In addition, the Fe–Y zeolites are about an order of magnitude less active than Co- and Cu-Y zeolites (*14, 15*). The values found for the activation energies were consistent with the range of values for other catalysts that have been reported (*1, 2, 9, 21, 22*).

Catalytic Behavior in the Presence of Oxygen

Kinetic studies in the presence of 1.2% oxygen were carried out over a temperature range of 480 to 575 K with a gas mixture containing 400 ppm of both NO and NH_3 in He. The results for NO reduction rate, activation energies and TOF are summarized in Table 3.

Comparison of the kinetic data presented in Tables 2 and 3 demonstrates that the presence of O_2 enhances the catalytic activity by approximately 2 orders of magnitude. This result is in agreement with previous studies (*1, 3, 5, 9, 23*). These data also show that the zeolite Si/Al ratio has only a modest effect on the catalytic activity, with the material having a Si/Al ratio of 3.2 being the most active. In addition, the TOF values compare favorably with that reported for iron oxide (*5*).

TABLE 3

Catalytic Activities for Fe–Y Zeolites in the Presence of O_2

Si/Al ratio	Rate[a]	TOF[b]	E_{ACT}[c]
2.4	9.6×10^{16}	1.3×10^{-4}	47.0[d]
3.2	1.8×10^{17}	3.2×10^{-4}	50.4[e]
4.4	5.8×10^{16}	1.3×10^{-4}	73.3[f]

[a] Estimated at 523 K, 400 ppm NO, 400 ppm NH_3 and 1% O_2. Units of molecules of NO/g of catalyst/s.

[b] Estimated at 523 K, 400 ppm NO, 400 ppm NH_3 and 1% O_2. Units of molecules of NO/Fe cation/s.

[c] Activation Energy (kJ/mol).

[d] Temperature range of 480–565 K.

[e] Temperature range of 480–575 K.

[f] Temperature range of 480–565 K.

TABLE 4

Kinetic Orders of NO and NH_3 for the NO–NH_3 Reaction over Fe–Y Zeolites in the Presence of O_2

Si/Al ratio	m^a	$T_m{}^b$	n^c	$T_n{}^d$
2.4	0.9	490	0.0	490
	0.9	540	0.3	542
3.2	1.7	490		
	1.5	502	0.1	503
	1.0	544	−0.2	542
4.4	1.0	493	0.0	493
	0.8	544	−0.4	544

[a] Kinetic order of NO.

[b] Temperature (K) at which the kinetic order of NO was determined.

[c] Kinetic order of NH_3.

[d] Temperature (K) at which the kinetic order of NH_3 was determined.

The kinetic orders with respect to NO and NH_3 were determined in the temperature range from 490 to 545 K. The results of these studies are presented in Table 4. The data show that the reaction was near first order in NO (0.8–1.0), in agreement with other studies (*1, 2, 4, 5, 9, 24, 25*). However, the lower temperature data (490–502 K) from the zeolite having a Si/Al ratio of 3.2 showed a higher order (1.7), decreasing to first order at higher temperature. The reaction rate was independent of the NH_3 concentration at low temperatures (490–500), in agreement with most of the literature results for other catalyst systems (*1–5, 9, 21, 24*). At 545 K, the order in NH_3 became slightly positive for the Si/Al = 2.4 zeolite, whereas it became slightly negative for the higher Si/Al samples.

The reaction stoichiometry dictates that the rates of NO and NH_3 consumption should be equal (i.e., $4NO + 4NH_3 + O_2 \rightarrow 4N_2 + 6H_2O$). This 1 : 1 NO : NH_3 consumption ratio was found at 480 K for the samples with an Si/Al ratio of 2.4 and 3.2. However, the consumption rate of NH_3 exceeded that of NO by a factor of nearly 2 at higher temperatures (565 K). This behavior suggests that NH_3 oxidation may play a significant role at higher temperatures.

The oxidation of ammonia by O_2 over the Fe–Y zeolites was studied using a mixture of approximately 400 ppm NH_3 and 1.2% O_2 in He at 493 and 543 K. None of the zeolites tested exhibited measurable ammonia oxidation activity at 493 K. The 4.4 Si/Al ratio zeolite was inactive at temperatures up to 543 K. The Fe–Y zeolites with Si/Al ratios of 2.4 and 3.2, however, showed measureable activity at 543 K, with rates of NH_3 consumption equal to 1.4×10^{17} and 1.0×10^{17} molecules of NH_3/g/s, respectively. The difference between the ammonia consumption rates and the NO consumption rates during SCR in the presence of oxygen was 1.6×10^{17} and 1.1×10^{17} molecules/g/s for these same zeolites, under similar conditions. The good agreement between the numbers for excess ammonia consumption during SCR and the rates of ammonia oxidation is consistent with the hypothesis that the excess ammonia consumption is due to ammonia oxidation.

Nitrous oxide was found to be a product of SCR in the presence of O_2. A 30% selectivity towards N_2O was observed at 493 K over a 2.4 Si/Al Fe–Y zeolite, in agreement with other reports (*10, 11*). The rate of N_2O formation was nearly equal to the rate of NO consumption at 593 K. Il'chenko and Golodets (*26*) reported that N_2O is produced by NH_3 oxidation. However, our 4.4 Si/Al Fe–Y sample showed NO consumption rates greater than NH_3 consumption rates over the entire range of conditions explored. This result is consistent with NO contributing to N_2O formation in addition to NH_3 being a source for its formation. The extents to which each molecule contributes over the range of Si/Al ratios and conditions studied are beyond the limits of the data reported herein.

Adsorption of NO

The interaction of NO with metal oxides and ion-exchanged zeolites is generally stronger after reduction (e.g., (*27–31*); how-

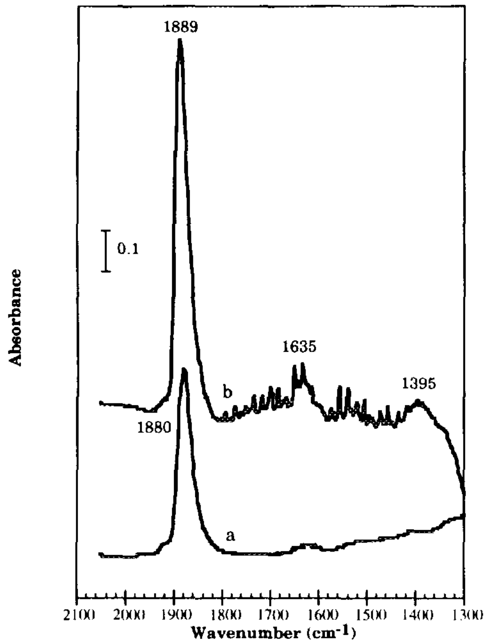

FIG. 1. *In situ* infrared spectra of an Fe–Y zeolite with a Si/Al ratio equal to 4.4, collected in a flowing 1000 ppm NO in He mixture at steady state (a) at 573 K and (b) at room temperature following standard oxidation.

ever, adsorption of NO has been reported on oxidized surfaces (*29*). *In situ* infrared spectra of the Fe–Y zeolite catalysts were collected in a flowing 1000 ppm NO diluted in He mixture at 300 and 573 K following oxidation (Fig. 1) and reduction (Fig. 2) treatments at 673 K. These figures are for an Fe–Y sample with a Si/Al ratio equal to 4.4, and they are representative of the spectra obtained with all Fe–Y zeolites. The dominant feature in these spectra is a band at 1870–1890 cm^{-1}, which is present only in the Fe–Y zeolite samples. This band has previously (*29*, *32*) been assigned to a mononitrosyl iron species either in a zeolite or on supported iron oxide. The band intensity is strongly enhanced upon reduction prior to NO exposure. The band is present, however, upon exposure of NO to samples which have undergone oxidation in flowing oxygen at 673 K. This behavior is especially true for Fe–Y zeolites with a high Si/Al ratio. Mössbauer spectroscopy (*19*) has shown that the Fe–Y zeolite with a 4.4 Si/Al ratio retains Fe^{2+}, even after extensive oxidation treatment at 673 K. Thus, at least in part, the band on the oxidized sample (Fig. 1) may be due to NO on Fe^{2+} cations remaining in the sample.

Several weak bands are observed in the room temperature spectra of Figs. 1 and 2 which can be assigned to nitrate species. Spectra collected at 523 K do not include these bands, probably due to the poor thermal stability of the nitrate species. When freshly oxidized Fe–Y zeolites were exposed to flowing 1000 ppm NO in He at 523 K, bands were observed at 1597 and 1628 cm^{-1} that increased in intensity for about 3 min and then decreased thereafter. These bands are most likely the result of gaseous NO$_2$ formed by reaction between gaseous NO and weakly adsorbed oxygen.

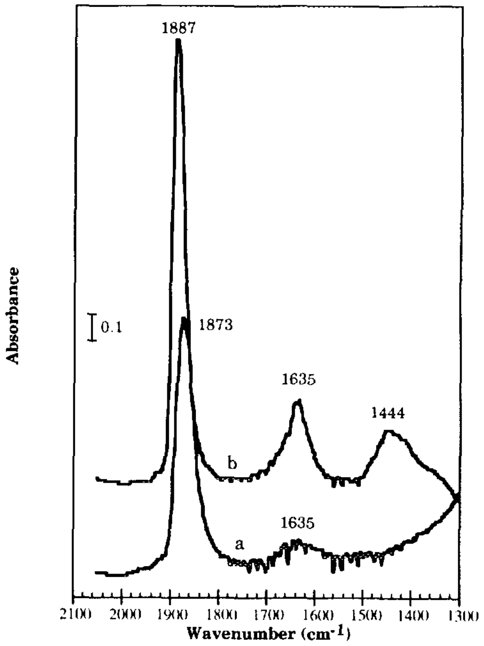

FIG. 2. *In situ* infrared spectra of an Fe–Y zeolite with a Si/Al ratio equal to 4.4, collected in a flowing 1000 ppm NO in He mixture at steady state (a) at 523 K and (b) at room temperature following standard reduction.

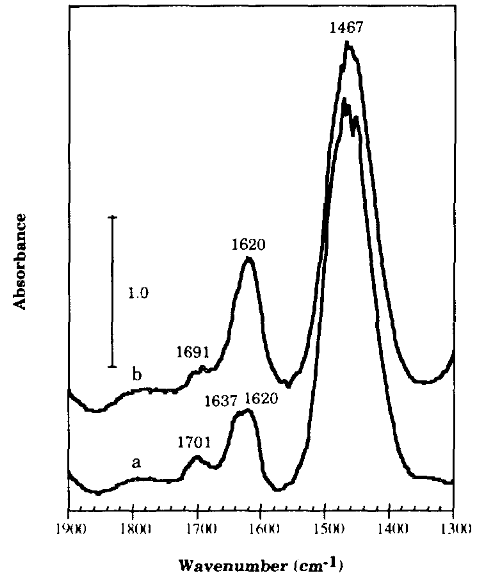

FIG. 3. Infrared spectra of an Fe–Y zeolite with a Si/Al ratio equal to 4.4, collected in a flowing 1000 ppm NH_3 in He mixture at room temperature following a standard (a) oxidation and (b) reduction treatment.

Adsorption of Ammonia

Bands due to the antisymmetric bending of the ammonium ion appear between 1500 and 1400 cm^{-1} (e.g., (*15*, *17*, *33–36*)). The symmetric bending mode, between 1700 and 1650 cm^{-1}, is IR inactive in unperturbed NH_4^+. The presence of H-bonding between NH_4^+ and the surface, however, distorts the molecule and lowers its T_d symmetry towards C_{3v}, thereby allowing the detection of this band in zeolites, as observed by others (*35*, *46*). Bands in the 1600-cm^{-1} region can be ascribed to the symmetric bending modes of adsorbed NH_3 while the antisymmetric modes are below the 1300-cm^{-1} detector cut-off. Finally, bond bending modes of NH_2 and NH species appear between 1600 and 1400 cm^{-1} (e.g., (*37–40*)).

The infrared spectra of an Fe–Y zeolite with a Si/Al ratio of 4.4, collected in flowing 1000 ppm NH_3 in He at ambient temperature following oxidation and reduction treatments at 673 K are shown in Fig. 3. The bands near 1465 and 1700 cm^{-1} can be assigned to the antisymmetric and symmetric bending modes of NH_4^+ adsorbed on Brønsted acid sites. The band at 1620 cm^{-1} can be assigned to the antisymmetric bending mode of NH_3 adsorbed on Lewis acid sites. The intensity of this band was stronger in the reduced sample, in agreement with the lower degree of coordination of Fe^{2+}, making these cations more accessible. The intensity of the band due to NH_4^+ remains essentially the same, or perhaps decreases slightly, when the sample is reduced. Therefore, additional Brønsted acid sites are not created upon reduction of the sample (as might be expected if the reduction reaction were written as $H_2 + 2Fe^{3+} \rightarrow 2Fe^{2+} + 2H^+$); and the charge balance on the lattice during reduction is preserved by removal of oxygen anions (e.g., $H_2 + 2Fe^{3+} + O^{2-} \rightarrow 2Fe^{2+}\ H_2O$). Finally, the band at 1637 cm^{-1} can be attributed to weakly bonded ammonia (*33*, *41*) or to adsorbed water.

Heating an Fe–Y sample in flowing He which had first been saturated with NH_3, caused the band near 1640 cm^{-1} to disappear at temperatures between 423 and 473 K, as demonstrated in Fig. 4 for the zeolite with a 2.4 Si/Al ratio. This behavior is consistent with the band being assigned to a weakly bound NH_3 species or to adsorbed H_2O. The disappearance of this band clearly revealed the band near 1615 cm^{-1} which is a strongly bound NH_3 species on Lewis acid sites.

Among the bands assigned to NH_4^+ on Brønsted acid sites, the band at 1505 cm^{-1} disappeared with a concomitant increase in the 1465-cm^{-1} band, upon heating from 323 to 373 K. These bands are probably associated with NH_4^+ on weak and strong Brønsted acid sites. Another band at 1695 cm^{-1} can be assigned to the symmetric bending mode of an NH_4^+ species. This latter band is present in ambient temperature spectra but disappeared upon heating (Fig. 4). Among the species discussed above, only NH_4^+ on Brønsted sites and NH_3 on Lewis sites were observable at 523 K. These species are, therefore, the

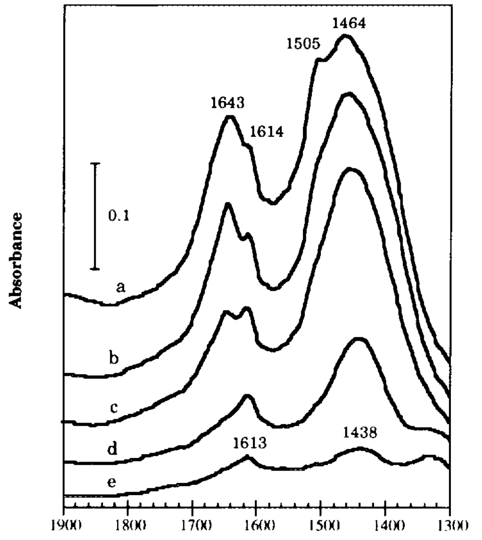

FIG. 4. *In situ* infrared spectra of an initially oxidized Fe–Y zeolite with a Si/Al ratio equal to 2.4, saturated with NH_3 at room temperature and heated in flowing He at (a) 323 K (1 h), (b) 373 K (40 min), (c) 423 K (30 min), (d) 473 K (1 h), and (e) 523 K (15 min).

ones expected to play a role in the SCR reaction.

Interaction of Fe–Y Zeolites with NO–NH_3–O_2 Mixtures

In situ IR spectra of an initially oxidized Fe–Y zeolite with a Si/Al ratio of 2.4 are presented in Fig. 5. The spectra were collected under steady-state reaction conditions at 523 K using different concentrations of NO and NH_3 in the presence of 1% O_2. The intensities of the two bands corresponding to NH_3 and NH_4^+ on Lewis and Brønsted acid sites vary in relationship to the NH_3 concentration in the gas phase. No detectable bands are present in the mononitrosyl region of the spectra (1900 − 1800 cm^{-1}) at low NO concentrations (Fig. 5c). However, at high concentrations (Fig. 5a) a weak band is present, and the intermediate spectra contain some indications for the presence of a mononitrosyl band. The mononitrosyl species is probably associated with the 15% of Fe^{2+} present as under these conditions, as shown by Mössbauer spectroscopy (*19*).

The effect of reaction temperature on the steady state surface concentrations of NH_3 and NH_4^+ species is shown in Fig. 6. The band intensities decrease with increasing temperature. Assuming the adsorption of these species follows a Langmuir isotherm, an estimate of the heats of adsorption can be made. The values for both NH_3 and NH_4^+ were nearly identical. The standard entropy and enthalpy changes of adsorption were found to be −185 J/mol-K and −130 kJ/mol, respectively. These values are within the range expected from calorimetric NH_3 adsorption measurements on various Y-zeolites (*42*).

In situ infrared spectra of the selective reduction of NO by NH_3 were also collected in the absence of oxygen. Mössbauer spectroscopy has shown that there is a slow re-

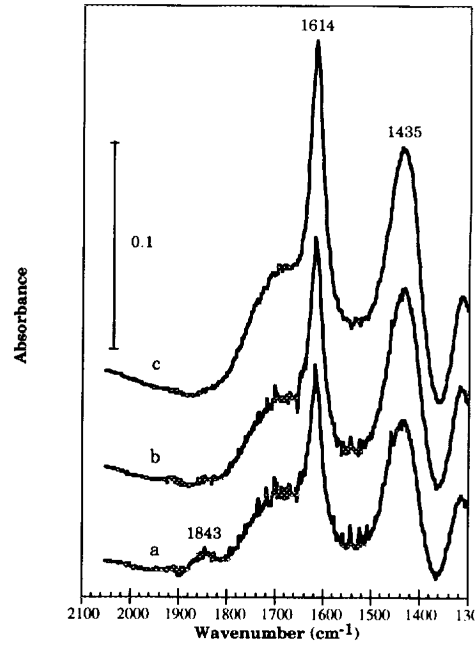

FIG. 5. *In situ* infrared spectra of an initially oxidized Fe–Y zeolite with a Si/Al ratio equal to 2.4 at steady state at 523 K with a flowing mixture of (a) 600 ppm NO, 200 ppm NH_3, 1% O_2 in He; (b) 400 ppm NO, 400 ppm NH_3, 1% O_2 in He; and (c) 200 ppm NO, 600 ppm NH_3, 1% O_2 in He.

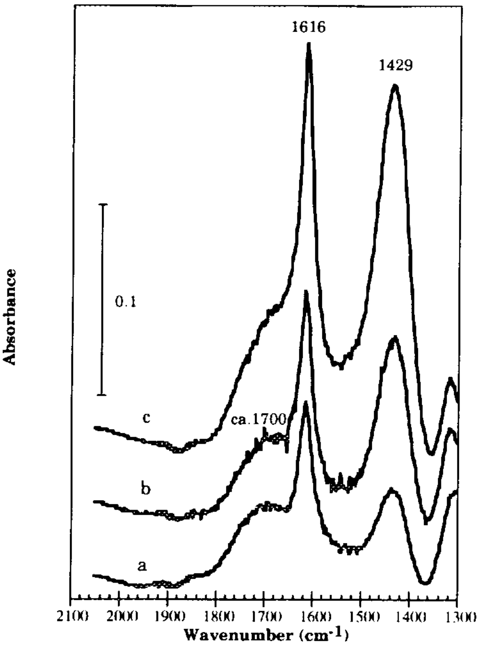

FIG. 6. *In situ* infrared spectra of an initially oxidized Fe–Y zeolite with a Si/Al ratio equal to 2.4 at steady state with a flowing mixture of 400 ppm NO, 400 ppm NH_3, 1% O_2 in He, at (a) 548 K, (b) 523 K, and (c) 498 K.

duction of the ferric to ferrous cations under these conditions (*19*), and our kinetic studies reported above showed a substantial decrease in catalytic activity starting with a fully oxidized catalyst. From the data shown in Fig. 7, it is seen that the amount of NH_3 which is adsorbed on the Lewis acid sites increases with increasing time, while there is a decrease in the concentration of NH_4^+ species. This behavior is consistent with the spectra of Fig. 3, indicating that the sample becomes reduced under reaction conditions in the absence of O_2. We also observed the same effect upon removing O_2 from a NO-NH_3-O_2 mixture at 523 K.

In situ IR spectra were obtained on a 2.4 Si/Al sample under 700 ppm flowing NH_3 and 1.6% O_2 in He at 523 and 548 K. These are experimental conditions under which NH_3 oxidation becomes an important side reaction. These spectra show increased intensity in the region between 1500 and 1600 cm^{-1} where NH and NH_2 species are found (*37–40*). However, it was not possible to resolve these bands from those of water or the strong NH_3 and NH_4^+ bands. Importantly, new bands appeared in the OH stretching region when the temperature was increased. Because hydroxyl groups are the product of NH_3 dehydrogenation, this observation supports the idea that ammonia oxidation proceeds through NH_2/NH species.

Reactivity Studies

Infrared spectra were collected versus time for a sample which had been equilibrated with a 1000 ppm NH_3 in He mixture at 523 K and subsequently exposed to different gas mixtures at this same temperature. Figures 8–10 show the spectra of a sample with a 2.4 Si/Al ratio collected when

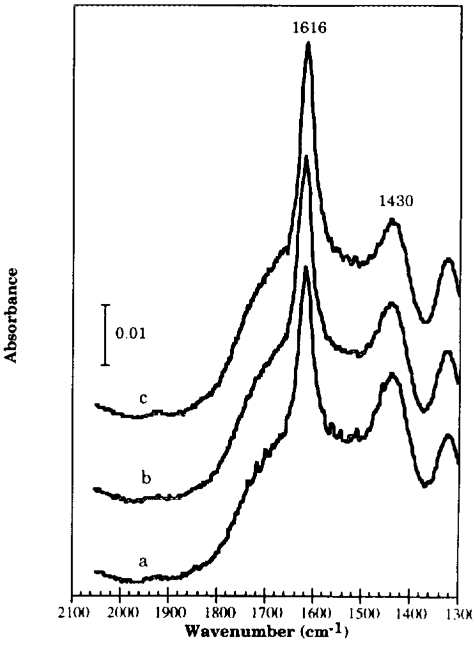

FIG. 7. *In situ* infrared spectra of an initially oxidized Fe–Y zeolite with a Si/Al ratio equal to 2.4 collected at 523 K in a flowing mixture of 500 ppm NO, 500 ppm NH_3 in He, (a) 1 h, (b) 2 h, and (c) 6.5 h after the introduction of the mixture.

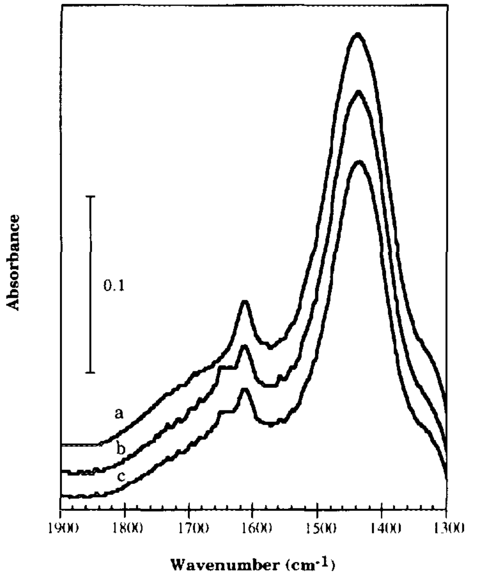

FIG. 8. *In situ* infrared spectra of an initially oxidized Fe–Y zeolite with a Si/Al ratio equal to 2.4 collected at 523 K (a) following 30 min in 1000 ppm NH_3 in He, (b) 10 min after the NH_3 in He has been replaced by He, and (c) 30 min after the replacement.

the gas was switched to (1) He, (2) a 5% O_2 in He mixture, and (3) a 1000 ppm NO in He mixture. Upon switching to pure He the IR bands due to NH_3 and NH_4^+ decreased slightly as small amounts of ammonia desorbed (Fig. 8). When the mixture was switched to the O_2 mixture, the NH_3 and NH_4^+ band intensity also decreased slightly (Fig. 9). This behavior is consistent with the kinetic results which demonstrate that NH_3 oxidation is not a major side reaction at these conditions. The band was formed near 1640 cm^{-1} can be assigned to water present in the He or to water formed from ammonia oxidation.

Importantly, when a 1000 ppm NO in He mixture is passed over an Fe–Y zeolite containing preadsorbed ammonia, the rate of disappearance of NH_3 and NH_4^+ bands was significantly higher than during treatments in either pure He or O_2 in He. Specifically, both the NH_3 and NH_4^+ bands were essentially eliminated within 30 min after the NO mixture was introduced, as shown in Fig. 10. Furthermore, the bands due to adsorbed ammonia were not replaced by bands due to adsorbed nitric oxide. In addition, a significant amount of water was produced from the reaction of NO with NH_3, as detected by the 1640-cm^{-1} band. Therefore, the disappearance in the IR spectrum of adsorbed ammonia is caused by reaction with nitric oxide, in contrast to displacement of ammonia by nitric oxide on the surface. When these experiments were repeated with an Fe–Y sample having a 4.4 Si/Al ratio, very similar results were obtained. These results are consistent with both NH_3 and NH_4^+ being involved in the NO reduction mechanism and the lack of any significant kinetic dependence on the Si/Al ratio.

When the above experiment was repeated using a NaH–Y sample having a 2.4 Si/Al ratio the intensity of the band due to NH_4^+ species did not decrease significantly in either flowing He or the O_2 in He mixture at 523 K. Furthermore, the intensity of the band due to NH_4^+ species on NaH–Y de-

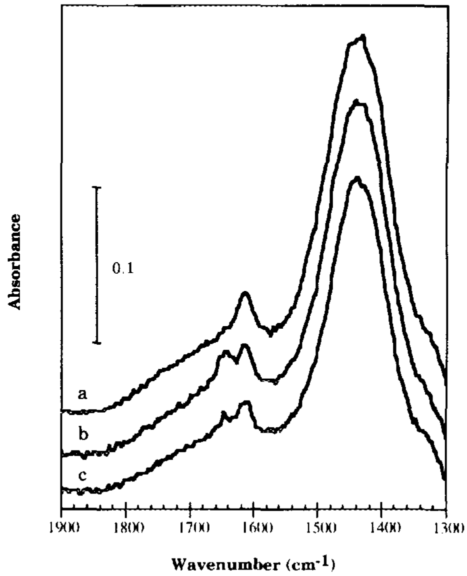

FIG. 9. *In situ* infrared spectra of an initially oxidized Fe–Y zeolite with a Si/Al ratio equal to 2.4 collected at 523 K (a) following 30 min in 1000 ppm NH_3 in He, (b) 10 min after the NH_3 in He has been replaced by 5% O_2 in He, and (c) 30 min after the replacement.

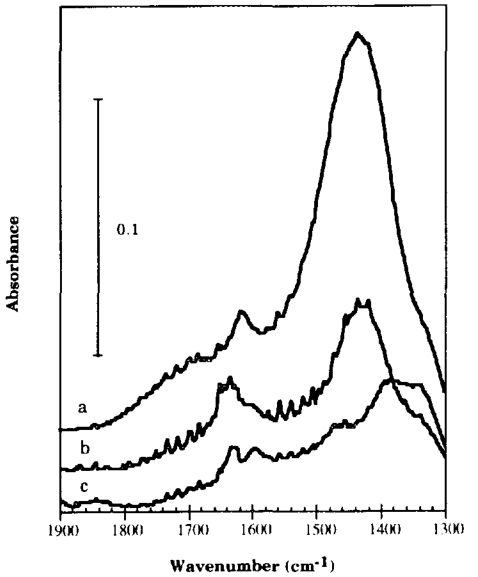

FIG. 10. *In situ* infrared spectra of an initially oxidized Fe–Y zeolite with a Si/Al ratio equal to 2.4 collected at 523 K (a) following 30 min in 1000 ppm NH_3 in He, (b) 10 min after the NH_3 in He has been replaced by 1000 ppm NO in He, and (c) 30 min after the replacement.

creased in the flowing NO in He mixture at approximately the same rate as observed in Fig. 10 for the Fe–Y zeolite sample at 523 K. This surprising result establishes that the rate of NO reaction with adsorbed ammonia over a fresh sample is comparable for the NaH–Y and Fe–Y zeolite samples.

DISCUSSION

The *in situ* infrared spectra presented here are consistent with only minimal amounts of NO being present on the Fe–Y zeolites under typical reaction conditions used for the selective reduction of nitric oxide by ammonia. In particular, adsorbed NH_3 and NH_4^+ species on Lewis and Brønsted acid sites, respectively, react with flowing NO without the appearance of IR bands corresponding to adsorbed nitrosyl species. Hence, we believe that the NO-NH_3 reaction over Fe–Y zeolites proceeds formally via reaction between adsorbed ammonia (both the NH_3 and NH_4^+ species) and either gas phase NO or weakly adsorbed NO. This reaction step may take place via formation of a short-lived iron nitrosyl species, with the steady-state concentration of this species being below the detectability limits of our IR experiments. Finally, the dominant coverage of NH_3 on the surface is also consistent with the lack of dependence of the rate expression on the ammonia concentration.

Following the reaction between NO and the NH_3 and NH_4^+ species, surface hydroxyls are formed. The removal of these species is required to complete the catalytic cycle. The ability of the iron cations to undergo oxidation–reduction is intimately linked with the catalytic cycle, especially within a zeolite framework. The formation of hydroxyl groups may also be associated with the charge balancing of the lattice brought about by the reduction of the Fe^{3+} cations.

In the absence of gas phase O_2, the NO must serve as the oxidizing agent for the Fe^{2+} cations. An additional possibility for the oxidizing agent is N_2O formed in the reaction between NO and NH_3 (*43, 44*). At steady state in the absence of O_2, the working catalyst has been shown to be nearly fully reduced (*19*). Furthermore, under these conditions the catalyst is nearly two orders of magnitude less active than when O_2 is present in the gas phase. These results are consistent both with NO being a poor oxidizing agent and the reaction being limited by the rate of reoxidation in the absence of oxygen. The fact that N_2O does not significantly improve the rate of reoxidation is consistent with it being a minor reaction product, since it is generally regarded as a better oxidizing agent than O_2.

Earlier Mössbauer spectroscopy studies at 523 K under comparable NO and NH_3 partial pressures and in the presence of O_2 (*19*) showed that the rate of Fe^{3+} reduction to Fe^{2+} was an order of magnitude slower than the steady-state SCR rate. This comparison of rates would seem to suggest that the oxidation–reduction properties of iron and the SCR reaction rates are unrelated.

However, we have previously shown that the rate of reduction of iron cations is highly dependent on the fraction of iron already reduced and on the Si/Al ratio of the zeolite (*43*). Both of these parameters are related to the lattice site that is occupied the highest fraction of time by the iron cations (since earlier studies have revealed that the cations move within the lattice at reaction temperatures). Thus, iron cations which are more accessible are more easily reduced than those in the hexagonal prisms, presumably because it is difficult for cations at these latter sites to move to more accessible locations. The difference in reduction rate for the various Fe^{3+} cations exceeds the order of magnitude difference between the overall reduction rate and the steady state SCR rate reported here. Therefore, these data suggest that only a fraction of the Fe cations are likely to be responsible for the SCR activity of the Fe–Y zeolite catalysts.

The reaction kinetics in the presence of oxygen show that the order in NO is unity and that the order in ammonia is zero. At higher temperatures the ammonia order may deviate slightly from zero and at the higher temperatures the deviation may also be a weak function of the zeolite Si/Al ratio. These results indicate that NO is involved in the rate-determining state. Unfortunately, these data do not provide information about the role of ammonia, because the surface is largely saturated with ammonia and the NO does not effectively compete with the ammonia for adsorption sites. While in the absence of oxygen the rate-determining step appears to be reoxidation of the iron, no dependence on oxygen was found in the presence of approximately tenfold excess of oxygen. This behavior is consistent with *in situ* Mössbauer spectroscopic results (*19*) which showed no detectable change in the oxidation states as a function of oxygen pressure.

With low Si/Al ratio zeolites, the order in ammonia becomes slightly positive at higher temperatures, indicating the reaction is moving towards second order and that reaction between NO and ammonia derived species is involved in the rate-determining step. With higher Si/Al ratio zeolites, the order becomes slightly negative at higher temperature. In conjunction with this inverse dependence on ammonia, the reduction of NO to N_2O becomes an important side reaction. This side reaction is expected to have an inverse dependence on ammonia if the mechanism for its formation from two NO molecules involves a dinitrosyl species.

There have been suggestions that NO_2 is an important species in these reactions (*45–48*). In our case, we do observe NO_2 formation upon exposure of NO to a freshly oxidized Fe–Y zeolite. It is likely, however, that the gaseous NO_2 formed in our experiments involved some residual O_2 species weakly adsorbed on the catalyst, since gas-phase reactions of NO with oxygen species are well known and facile.

Ammonia Oxidation

The kinetic studies provide evidence that oxidation of ammonia by oxygen commences near 523 K and becomes increasingly dominant as the temperature increases. The *in situ* infrared spectra suggest that either adsorbed NH_2 or NH, which are formed only when iron is in the zeolite, are important intermediates in the reaction pathway. Furthermore, *in situ* Mössbauer studies indicate that the oxidation state of the Fe–Y catalysts in $NO:NH_3:O_2$ gas mixtures is more highly reduced for higher Si/Al ratios at high $NO:NH_3$ ratios (*19*). With increasing Si/Al ratio of the catalyst, the fraction of iron in the fully oxidized state decreases and as a result the amount of extraframework oxygen species decreases. If this extraframework oxygen is necessary for the dehydrogenation of the NH_2 species, then it would be expected that the rate of ammonia oxidation would decrease as the overall oxidation state of the iron decreases.

While the kinetic results indicate iron cations are necessary for zeolites to exhibit steady-state catalytic activity for the

$NO-NH_3$ reaction in the presence of O_2, infrared results from the reaction of NO with preadsorbed ammonia demonstrate that NH_4^+ species adsorbed on a NaH–Y zeolite react with NO, even though iron cations are not present in the catalyst in appreciable concentration. This observation suggests that the presence of iron cations is not necessary, at least for the initial reaction of NH_4^+ with NO. The iron cations in the zeolites function catalytically by undergoing oxidation–reduction cycles. The mechanism operating in the NaH–Y catalyst does not contain cations able to undergo oxidation–reduction, and this catalyst must carry out the NO reduction by a different mechanism. In this respect, it has been suggested that the catalytic cycle for the SCR reaction in zeolites may involve reaction between NO and H atoms (*14*, *15*). In this case, the rate-determining step in the catalytic cycle may be the formation of HNO species and the subsequent production of N_2O. Our steady-state kinetic experiments suggest that this reaction is a significantly slower process under the conditions studied.

CONCLUSIONS

Fe–Y zeolites are active for the selective reduction of nitric oxide by ammonia both in the presence and absence of O_2. Although they are not as active as V_2O_5 catalysts, their activity is comparable to Fe_2O_3 catalysts. Deactivation of initially oxidized catalysts was observed when O_2 was absent from the gas phase. In the presence of gas phase O_2, the steady-state rate is enhanced by about two orders of magnitude. The presence of Fe cations in the zeolites is necessary to sustain steady state catalytic activity.

The SCR reaction was found to be first order in NO. The kinetic order with respect to ammonia was essentially zero at temperatures up to 545 K, whereupon it deviated either higher or lower depending on the Si/Al ratio of the Fe–Y zeolite. The negative deviation may be related to the onset of NO reduction to N_2O, where ammonia would act as a site blocking agent. The positive deviation may be related to the onset of ammonia oxidation or more simply to a decrease in the ammonia surface coverage with increasing temperature. One of the interesting questions identified in this study is why the selectivity of these side reactions depends so strongly on the Si/Al ratio of the Fe–Y zeolite.

The rate-limiting step in the catalytic reduction of nitric oxide in the presence of O_2 appears to be the reaction between adsorbed ammonia and either gaseous NO or a NO surface species which is in such low concentration that it is not visible in the IR spectra. The catalytic cycle involves the extraframework oxygen anions associated with the ferric cations. The NH_4^+ species adsorbed on a NaH–Y were found to react rapidly with NO in the absence of excess ammonia. In this case, the rate-determining step in the catalytic cycle may be the formation of HNO species and the subsequent production of N_2O. In the absence of O_2, the rate-determining step is the catalyst reoxidation by NO.

ACKNOWLEDGMENTS

The authors express their gratitude to the National Science Foundation for Grant CBT-8810149 which supported this work. In addition, we thank G. Yaluris (UW–Madison) for valuable discussions.

REFERENCES

1. Inomata, M., Miyamoto, A., and Murakami, Y., *J. Catal.* **62,** 140 (1990).

2. Miyamoto, A., Kobayashi, K., Inomata, M., and Murakami, Y., *J. Phys. Chem.* **86,** 2945 (1982).

3. Odenbrand, C. U. I., Lundin, S. T., and Andersson, L. A. H., *Appl. Catal.* **18,** 335 (1982).

4. Wong, W. C., and Nobe, K., *Ind. Eng. Chem. Prod. Res. Dev.* **23,** 564 (1984).

5. Wong, W. C., and Nobe, K., *Ind. Eng. Chem. Prod. Res. Dev.* **25,** 179 (1986).

6. Nam, I.-S., Eldridge, J. W., and Kittrell, J. R., *Ind. Eng. Chem. Prod. Res. Dev.* **53,** 186 (1986).

7. Baiker, A., Dollenmeier, P., Glinski, M., and Reller, A., *Appl. Catal.* **35,** 351 (1987).

8. Bosch, H., and Janssen, F. J. J. G., *Catal. Today* **2,** 369 (1988).

9. Powell, D. E., and Nobe, K., *Chem. Eng. Commun.* **10,** 103 (1981).

10. Seiyama, T., Arakawa, T., Matsuda, T., Yamazoe, N., and Takita, Y., *Chem. Lett.*, 781 (1975).

11. Seiyama, T., Arakawa, T., Matsuda, T., and Takita, Y., *J. Catal.* **48,** 1 (1977).
12. Mizumoto, M., Yamazoe, N., and Seiyama, T., *J. Catal.* **55,** 119 (1978).
13. Arakawa, T., Mizumoto, M., Takita, Y., Yamazoe, N., and Seiyama, T., *Bull. Chem. Soc. Jpn.* **50,** 1431 (1977).
14. Williamson, W. B., and Lunsford, J. H., *J. Phys. Chem.* **80,** 2664 (1976).
15. Iizuka, T., and Lunsford, J. H., *J. Am. Chem. Soc.* **100,** 6106 (1978).
16. Ramis, G., Busca, G., Lorenzelli, V., and Forzatti, P., *Appl. Catal.* **64,** 243 (1990).
17. Topsøe, N.-Y., *J. Catal.* **128,** 499 (1991).
18. Windhorst, K. A., and Lunsford, J. H., *J. Am. Chem. Soc.* **97,** 1407 (1975).
19. Schmidt, R., Amiridis, M. D., Dumesic, J. A., Zelewski, L. M., and Millman, W. S., *J. Phys. Chem.* **96,** 1407 (1992).
20. Delgass, W. N., Gartem, R. L., and Boudart, M., *J. Phys. Chem.* **73,** 2970 (1969).
21. Wu, S. C., and Nobe, K., *Ind. Eng. Chem. Prod. Res. Dev.* **16,** 136 (1977).
22. Miyaomoto, A., Medhanavyan, D., and Inui, T., *Chem. Express* **1,** 559 (1986).
23. Bosch, H., Janssen, F. J. J. G., van der Kerkhof, F. M. G., Oldenziel, J., van Ommen, J. G., and Ross, J. R. H., *Appl. Catal.* **25,** 239 (1986).
24. Czarnecki, L. J., and Anthony, R. G., *AICHE J.* **36,** 794 (1990).
25. Medros, F. G., Eldridge, J. W., and Kittrell, J. R., *Ind. Eng. Chem. Prod. Res. Dev.* **28,** 1171 (1989).
26. Il'chenko, N. I., and Golodets, G. I., *J. Catal.* **39,** 57 (1975).
27. Niiyama, H., and Echigoya, E., *J. Catal.* **38,** 238 (1975).
28. Davydov, A. A., and Lokhov, Y. A., *React. Kinet. Catal. Lett.* **8,** 47 (1978).
29. Segawa, K. Chen, Y., Kubsh, J. E., Delgass, W. N., Dumesic, J. A., and Hall, W. K., *J. Catal.* **76,** 112 (1982).
30. Gasior, M., Haber, J., Machej, T., and Czeppe, T., *J. Mol. Catal.* **43,** 359 (1988).
31. Li, Y., and Hall, W. K., *J. Catal.* **129,** 202 (1991).
32. Aparicio, L. M., Hall, W. K., Fang, S., Ulla, M. A., Millman, W. S., and Dumesic, J. A., *J. Catal.* **108,** 233 (1987).
33. Belokopytov, Y. V., Kholyavenko, K. M., and Bevei, S. V., *J. Catal.* **60,** 1 (1979).
34. Inomata, M., Mori, K., Miyamoto, A., Ui, T., and Murakami, Y., *J. Phys. Chem.* **87,** 754 (1983).
35. Uytterhoeven, J. B., Christner, L. G., and Hall, W. K., *J. Phys. Chem.* **69,** 2117 (1965).
36. Galuszka, J., Ceckeiwicz, S., and Baranski, A., *Trans. Faraday Soc.* **74,** 1150 (1978).
37. Kagami, S., Onishi, T., and Tamaru, K., *J. Chem. Soc. Faraday Trans.* **86,** 989 (1990).
38. Nakata, T., and Matsushita, S., *J. Phys. Chem.* **72,** 458 (1968).
39. Budneva, A. A., and Davydov, A. A., *React. Kinet. Catal. Lett.* **11,** 133 (1979).
40. Busca, G., Guidetti, R., and Lorenzelli, V., *J. Chem. Soc., Faraday Trans.* **86,** 989 (1990).
41. Morrow, B. A., and Cody, I. A., *J. Catal.* **45,** 151 (1976).
42. Cardona-Martinez, N., and Dumesic, J. A., *Adv. Catal.* **38,** 149 (1992).
43. Aparicio, L. M., Dumesic, J. A., Fang, S., Long, M. A., Ulla, M. A., Millman, W. S., and Hall, W. K., *J. Catal.* **104,** 381 (1987).
44. Aparicio, L. M., Ulla, M. A., Millman, W. S., and Dumesic, J. A., *J. Catal.* **110,** 330 (1988).
45. Takagi, M., Kawai, T., Soma, M., Onishi, T., and Tamaru, K., *J. Phys. Chem.* **80,** 430 (1976).
46. Takagi, M., Kawai, T., Soma, M., Onishi, T., and Tamaru, K., *J. Catal.* **50,** 441 (1977).
47. Kiovsky, J. R., Koradia, P. B., and Lim, C. T., *Ind. Eng. Chem. Prod. Res. Dev.* **19,** 218 (1980).
48. Brandin, J. G. M., Andersson, L. A. H., and Odenbrand, C. U. I., *Catal. Today* **4,** 187 (1989).